Eur. Phys. J. D **10**, 131–140 (2000)

THE EUROPEAN PHYSICAL JOURNAL D

EDP Sciences

Persistent spectral hole-burning in a Eu^{3+}-doped aluminosilicate glass from 8 to 295 K: Study of the burning and refilling kinetics, and of optical dephasing

W. Beck[a], A.Ya. Karasik[b], J. Arvanitidis[c], and D. Ricard[d]

Laboratoire d'Optique Quantique, École Polytechnique, 91128 Palaiseau, France

Received 28 July 1999

Abstract. High-temperature persistent spectral hole-burning (PSHB), up to room temperature, has been observed in a Eu^{3+}-doped aluminosilicate glass using a high peak-power nanosecond dye laser. Spontaneous refilling as well as thermal cycling measurements show that at least two mechanisms, a fast and a slow one, are involved in our sample. We suggest that the fast or "easy" component may correspond to a non-photochemical local rearrangement of the host or to photoreduction of the Eu^{3+} ions and that the second one leading to very stable photoproducts may correspond to transfer of an electron over a sizable distance through a several-step process. The mechanisms we suggest agree with light-induced hole refilling measurements. Line broadening mechanisms are discussed and the temperature-dependent part of the homogeneous width and of the spectral shift is interpreted in terms of a two-phonon (Raman) process involving pseudo-local phonons.

PACS. 32.70.Jz Line shapes, widths, and shifts – 63.20.Mt Phonon-defect interactions – 78.30.Ly Disordered solids

1 Introduction

Rare earth ions doped in solid matrices, either crystalline or amorphous, play an important role in laser physics. They have also been used as sensitive probes of the host properties [1]. When compared with crystals, glasses show for example unusual low-temperature thermal properties. Impurities, usually called chromophores, also show different optical properties when embedded in a glassy host as compared with crystalline matrices. *Via* the crystal field, each impurity is sensitive to its environment that modifies the central frequency of a given electronic transition. The great variety in the ions environments leads to a very broad inhomogeneous distribution. The dynamics of the host also lead to fast frequency modulation that may contribute to homogeneous broadening of the transition. A large amount of work has been devoted to the interpretation of the unusual low temperature properties of glasses, mainly in terms of low-energy excitations or two-level systems (TLS). A recent critical account on this may be found in [2]. Glasses also possess higher energy excitations that do not exist in crystals, the well-known "boson peak" whose exact origin is still being debated [3] and that may be involved in the process of line broadening at high enough temperature.

Another attractive feature of rare-earth ions is that some of them, Sm^{2+}, Eu^{3+}, Pr^{3+}, Nd^{3+}, have been observed to exhibit persistent spectral hole burning (PSHB) [4–6]. Since its first observation, PSHB has aroused a great interest because of its potential applications in the field of optical data storage or processing [7]. Its main advantage is that, adding the frequency dimension, it greatly enhances the storage density. The upper limit for the enhancement factor is the ratio of the global absorption linewidth of the transition under consideration to the hole spectral width. In the case of rare-earth ions, this ratio may be larger than 10^7 at low temperature. Recently, using an organic molecule doped in a polymer matrix, a storage density of at least 10^{10} bits per cm^2 has been demonstrated [8], which compares well with conventional memories. However, this PSHB result was obtained at 1.7 K. When the temperature is increased, two problems arise. First, the homogeneous linewidth increases whereas the inhomogeneous one remains practically unchanged. Second, the hole lifetime becomes very short and burning a persistent spectral hole at room temperature usually is a challenge.

[a] *Permanent address*: Department of Physics, University of California, Berkeley, CA 94720, USA.

[b] *On leave from*: General Physics Institute, 38 Vavilov Street, Moscow 117942, Russia.

[c] *On leave from*: Physics Department, Aristotle University of Thessaloniki, 54006 Thessaloniki, Greece.

[d] e-mail: `ricard@leonardo.polytechnique.fr`

The search for high temperature PSHB in rare-earth ion systems started with Sm^{2+}. The PSHB mechanism for this system is photoionization of Sm^{2+} into Sm^{3+}, followed by trapping of the ejected electron. The point mentioned above regarding the ratio between the linewidths was solved in this case by turning to mixed crystals or glasses that show a broader inhomogeneous distribution of optical centers: room-temperature PSHB was observed in mixed crystals [9–11] and in various glasses [12,13] doped with Sm^{2+}. PSHB had also been observed at low temperature in the case of Eu^{3+} [4]. The main advantage of the isoelectronic Sm^{2+} and Eu^{3+} ions is that the relevant transition, the $^7F_0$–$^5D_0$ one, takes place between nondegenerate levels (when the nuclear spin is neglected). The rare earth ions being usually trivalent, the problem with samarium is that although Sm^{2+} can be obtained by partial reduction, most of the samarium remains present in the host as Sm^{3+}. Hence the interest aroused by Eu^{3+}. PSHB up to 77 K was observed for this ion doped in an aluminosilicate (AlSi) glass prepared in the conventional way [14]. More recently, PSHB at room temperature was reported for the same ion doped in a sodium aluminosilicate glass [15], then in a sodium silicate glass [16] also prepared in the conventional way. In the meantime, PSHB in the Eu^{3+} ion had been observed up to 200 K in an AlSi glass prepared using the sol-gel technique [17].

In the present paper, we report on the observation of PSHB from 8 to 295 K in an AlSi glass sample very similar to the one used in [14] but using a high peak-power nanosecond dye laser. At room temperature, 5% deep, long-lived holes could be burned. Their saturated width of 3.2 cm^{-1} implies a lower bound of 50 for the ratio of the global linewidth of the absorption band to the hole width. Since understanding the PSHB mechanisms is crucial for the development of better storage media, we concentrated our efforts on studying the temperature and irradiation dose dependence of the hole depth and area, on the burning kinetics as well as on the refilling kinetics. Regarding refilling that is an important issue when thinking of applications, we considered both cases of spontaneous (or thermally-induced) hole refilling and of light-induced hole refilling.

Making use of PSHB, we also studied homogeneous line broadening mechanisms for the same transition in the same material: working near the peak of the line, we studied the temperature dependence of the homogeneous linewidth and of the frequency shift in the 8–60 K range. As already pointed out [18,19], PSHB allows one to measure both the linewidth and the frequency shift, lending further support to the interpretation.

This paper is organized in the following way. In Section 2, we give the experimental details regarding our sample and measurements. In Section 3, we report our main experimental results and we discuss them in Section 4, first comparing our material with those in which room-temperature PSHB has recently been observed for Eu^{3+}. In Section 4.1, after having shown that at least two mechanisms, a fast or "easy" and a slow one, are involved, we discuss what these mechanisms may be; together with already suggested processes such as photoinduced local rearrangement of the host or photoreduction that may correspond to the fast component(s), we suggest that the slow one is a three-step process whose result is the transfer of an electron over a sizable distance, a very stable modification. In Section 4.2 finally, we discuss the line broadening process. Whereas the TLS alluded to at the very beginning of this section are mainly operative at low temperature, the measurements performed above $\sim$ 10 K are often interpreted in different terms. We will compare our findings with previous results and interpretations. In our case, the temperature dependence points to a two-phonon (Raman) process involving pseudo-local phonons.

2 Experimental details

Our AlSi glass sample was an oxide glass with the following composition: 74.8 SiO_2, 22.0 Al_2O_3 and 3.2 Eu_2O_3 (mol%), *i.e.* the same chemical composition as the sample that was studied in [14]. The melt was prepared at high temperature under an argon atmosphere; *versus* helium in [14]. Most of the experiments relied on measurements of the fluorescence intensity, either as a function of the exciting laser frequency (fluorescence excitation spectroscopy) or as a function of time (kinetics). The most intense lines in the fluorescence spectrum being the ones corresponding to the $^5D_0$–$^7F_2$ transition around 612 nm, the fluorescence photons collected at 90° were filtered by a combination of Schott OG590 and RG610 filters and detected by a Philips XP2013 photomultiplier tube whose output was fed into a gated boxcar integrator, model SR250 from Stanford Research Instruments. The gate had a 100 μs delay with respect to the laser pulse and a 15 μs width. The signal was normalized and usually averaged over 50 laser shots.

The laser was a Continuum ND6000 nanosecond dye laser pumped by a frequency-doubled Q-switched Nd:YAG laser. Its repetition rate is 50 pulses per second, the pulse duration is 5 ns. The $^7F_0$–$^5D_0$ transition of Eu^{3+} taking place around 576 nm, we used rhodamine 590 as the dye. With a dual-grating arrangement for the oscillator, the dye laser spectral width, as measured using a Fabry-Perot etalon and averaging over 50 shots, was 0.05 cm^{-1} (1.5 GHz). The maximum average output power we used is 80 mW, but we often worked at much lower power: for example, a few microwatts were sufficient to burn a hole at low temperature. The laser beam was gently focused on the sample with a 50 cm focal-length lens leading to a beam waist of $\sim$ 100 μm diameter. An average power of 1 W thus translates into an average intensity of $\sim$ 125 W/mm^2 or a fluence of $\sim$ 2.5 J/mm^2 per pulse. In the following, we will only give the average intensity. The reading power (or intensity) was typically 100 to 1000 times weaker than the burning one.

For all the laser measurements, the sample was sitting in a cryo-refrigerator that allowed the sample temperature to be varied from 8 to 295 K. The sample thickness along the laser beam was $\sim$ 3 mm.

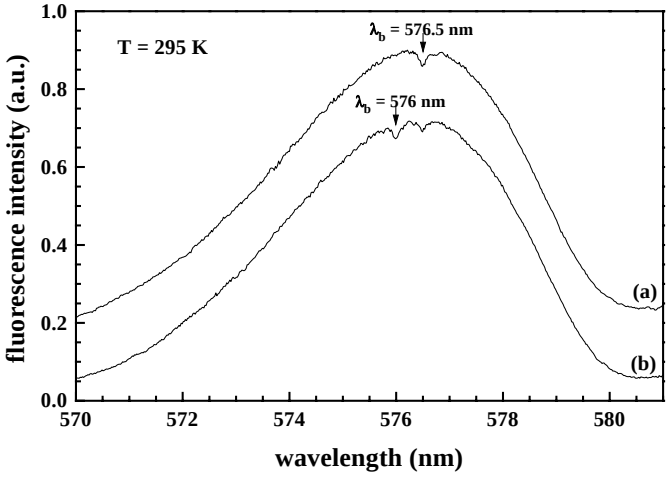

Fig. 1. Room-temperature fluorescence excitation spectra of our aluminosilicate glass doped with Eu^{3+} ions in the vicinity of the $^7F_0$–$^5D_0$ transition. Curve (a) shows a persistent spectral hole that was burned at room temperature with a laser beam of wavelength 576.5 nm. Curve (b) was obtained after a second irradiation at 576 nm and shows two persistent spectral holes. For the sake of clarity, curve (a) has been translated vertically.

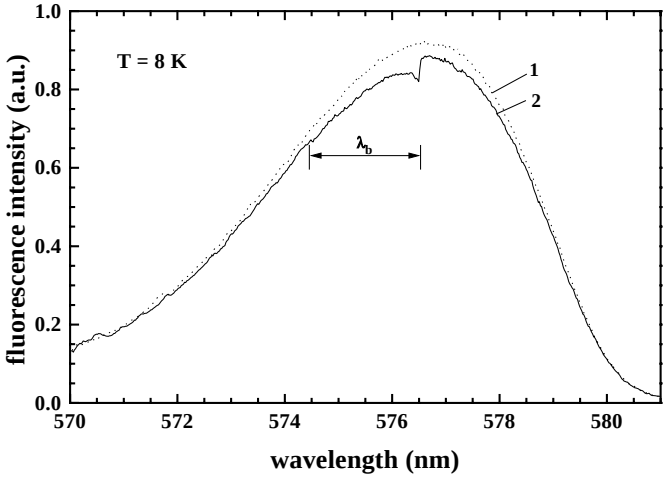

Fig. 2. Low temperature fluorescence excitation spectra for the same sample as in Figure 1. Curve 1, dotted line, was obtained before any bleaching. Curve 2, solid line, was recorded after irradiation with a pump beam whose wavelength was scanned from 574.5 to 576.5 nm at a scan speed of 0.005 nm/s.

3 Experimental results

We do not show here the room-temperature linear absorption spectrum of our sample since it is identical to the one reported in reference [14], Figure 1. The sample has a yellow color most probably due to the presence of a significant amount of Eu^{2+} ions that show a broad interconfigurational $4f$–$5d$ transition peaking around 420 nm. This fact is of importance since it shows that our AlSi host is electron donating and reduces part of the trivalent europium ions. This reducing ability is usually assigned to the presence of non-bonding oxygen ions. Superimposed on the low-energy trailing edge of this absorption band, lines due to intraconfigurational $4f$–$4f$ transitions of the Eu^{3+} ions may be observed. They correspond to the $^7F_0$–^5D_J transitions with $J = 0, 1$ and 2, in order of increasing intensity.

Curve (a) in Figure 1 shows the fluorescence excitation spectrum measured at room temperature (295 K) in the region of the $^7F_0$–$^5D_0$ transition after irradiation (also at room temperature) of the sample at $\lambda_b = 576.5$ nm for about 60 minutes with an average burning intensity $I_b = 5$ W/mm^2. A persistent spectral hole 5% deep is clearly observable. Its width (FWHM) is 3.2 cm^{-1}. Curve (b) shows the fluorescence excitation spectrum of the same spot after a second irradiation at $\lambda_b = 576$ nm with the same burning intensity but an irradiation time ten times shorter. A second spectral hole with the same depth as the one in curve (a) is observed. At the same time, we observe that burning of a second hole has led to partial refilling of the first one. We also note that the fact that the hole depth is the same in cases (a) and (b) is an indication of saturation. The 3.2 cm^{-1} width thus observed is an upper limit for the unsaturated hole width. The global absorption linewidth of the $^7F_0$–$^5D_0$ transition in our sample being ~ 150 cm^{-1}, the ratio of the global linewidth of the transition to the hole width as measured here is 50 and is expected to be larger when avoiding saturation.

Figure 2 shows the fluorescence excitation spectrum before, dotted line, and after, solid line, irradiation by a burning laser whose wavelength was scanned from 574.5 to 576.5 nm (with a scan-speed of 0.005 nm/s), both spectra being measured at 8 K. The burning laser intensity was 2.5 W/mm^2. Similarly to Figure 1, we see that bleaching is larger at the last burning wavelength. Again, irradiation at a new wavelength has led to partial refilling of the previously burned holes. Similarly to Figure 1 too, we see that the holes are not accompanied by anti-holes. The change in the absorption coefficient being larger at low temperature (spectral holes 20% deep could be burned), we also see in Figure 2 that, besides bleaching at the exciting laser wavelength, a smaller, non-frequency selective bleaching of the whole line takes place.

Figure 3 shows the results of a burning kinetics study performed at room temperature. The fluorescence intensity is measured as a function of time during exposure to the burning laser, the burning intensity being 1.25 W/mm^2. The solid line corresponds to a fit to the data, the model being the sum of an exponential term plus a constant. We see again that the hole depth saturates (in fact at a 4–5% level).

We studied spontaneous refilling by monitoring, immediately after the burning phase, the time dependence of the luminescence intensity excited by the read beam. The results obtained at room temperature are shown in Figure 4a. Similar measurements were performed at 8 K, the results being shown in Figure 4b. The data are fitted assuming the sum of two exponential components plus a constant. At low temperature, as can be seen in Figure 4b, the results indicate the presence of a slow component,

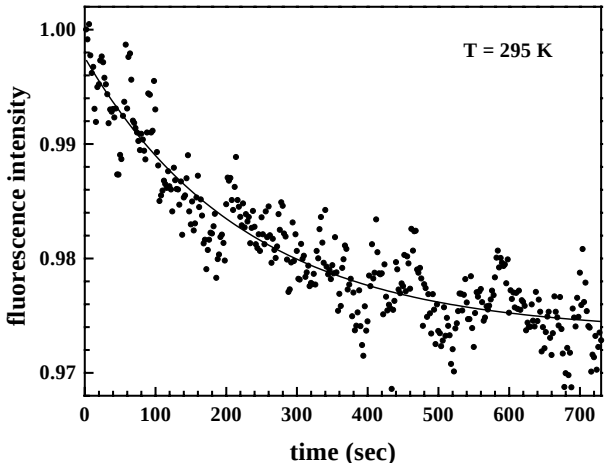

Fig. 3. Room-temperature burning kinetics studies: the fluorescence intensity (normalized to one at $t = 0$) was recorded as a function of time during the burning process. The burning wavelength was 576.5 nm, the average burning intensity 1.25 W/mm^2. The solid line is a fit to the data assuming the sum of an exponential term plus a constant.

of a fast one with a time constant of $\sim$ 70 minutes and of a faster one with a time constant of $\sim$ 6 minutes. At room temperature, Figure 4a, the time constant for the fast component is $\sim$ 2 hours; evidence for the faster component is less clear.

When studied as just described, spontaneous refilling may be perturbed by the constant presence of the reading beam. Another way to study it is to burn a hole at time $t = 0$, then to read it by scanning the read laser frequency 1 hour later, then 2 hours later, and so on. The hole area is then plotted as a function of the elapsed time. Since each scan only lasts a few minutes, this latter approach is less invasive. Figure 5 shows the results of a study of spontaneous hole refilling performed in this way at room temperature. They were fitted assuming the sum of an exponential component plus a constant. We observe that part of the hole (about two thirds) refills with a time constant of about 2 hours, the same value as the one we get for the time constant of the fast component in Figure 4a. Several days later however, a sizable fraction of the hole is still present; it corresponds to the slow component in Figure 4.

In order to better understand spontaneous hole refilling, temperature cycling measurements were performed. A hole was burned at 8 K, then its area was measured. The sample was then heated to 15 K for example, kept at this cycling temperature for a few minutes, then cooled back to 8 K, and the hole area was measured again. This process was repeated with a higher cycling temperature again and again, each time changing the laser spot on the sample. Figure 6 shows the corresponding results: the hole area normalized to its initial value is plotted as a function of the cycling temperature. We observe a "rapid" decrease of part of the hole below 40 K whereas the hole area remains practically constant above 50 K.

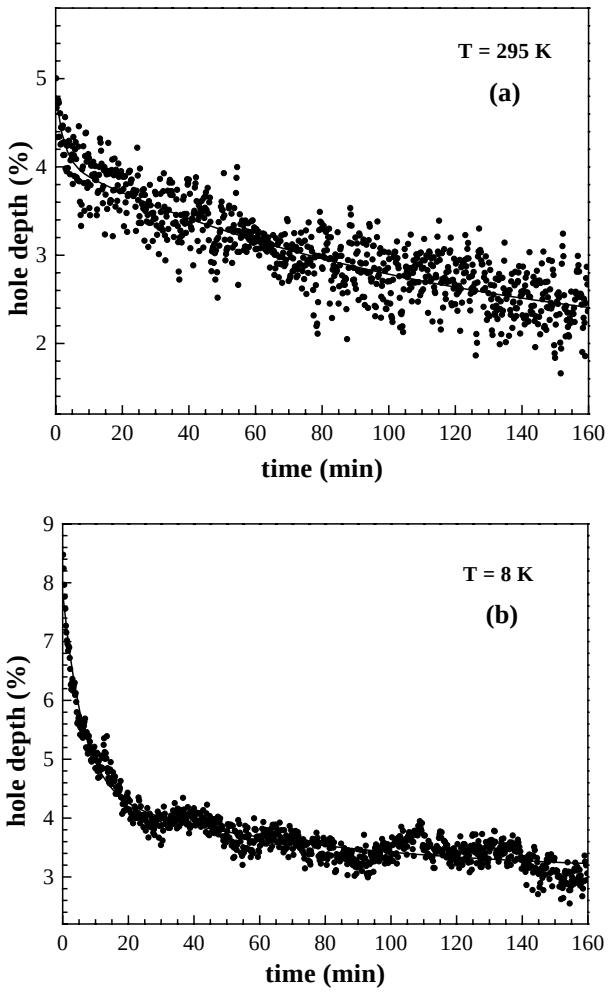

Fig. 4. Spontaneous hole refilling studies: the fluorescence intensity, later translated into hole depth, is recorded as a function of time immediately following the hole burning phase. The measurements were carried out at room temperature, part (a), and at low temperature, part (b). The solid lines are fits assuming the sum of two exponential terms plus a constant.

Light induced hole refilling is another important issue in optical data storage. In order to study light induced refilling, the sample is irradiated by a powerful laser beam at a given wavelength. The excitation spectrum is then recorded using a much weaker read beam. The same sample spot is then irradiated by a powerful laser beam at a second wavelength and the new excitation spectrum is then recorded and so on. The upper part of Figure 7 shows the results of such a study performed at 8 K. We plot minus the fluorescence intensity change as a function of the scanned wavelength of the read beam. We start burning a hole at 577 nm and read the spectrum: we thus get curve (a). We then burn a second hole at 576 nm, the sample position being unchanged, and read the spectrum again: we thus get curve (b). We go on, irradiating at 578 nm, curve (c), then at 576.5 nm, curve (d), and so on. We observe that burning a new hole partly refills previously burned ones. Regarding light-induced hole refilling,

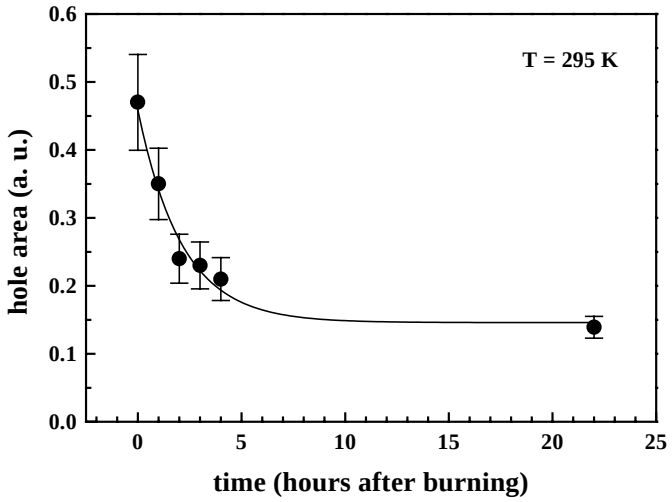

Fig. 5. Spontaneous hole refilling studies: a spectral hole is burned at $t = 0$, its area, as deduced from Lorentzian fits to the change in the fluorescence excitation spectra, is measured at $t = 0, 1, 2, 3, 4$ and 22 hours. The measurements were performed at room temperature. The solid line is a fit assuming the sum of an exponential term plus a constant.

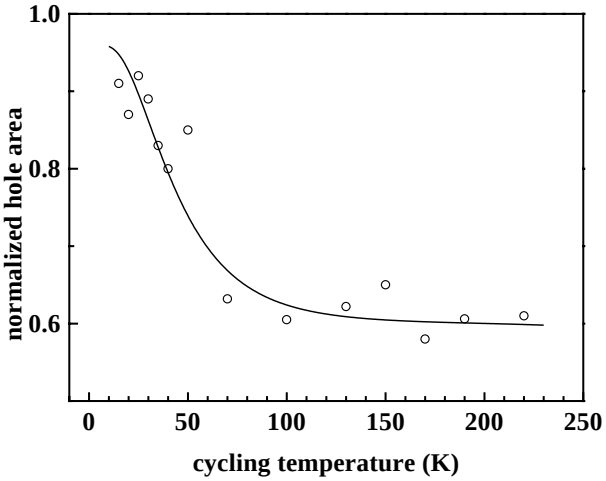

Fig. 6. Thermal cycling measurements. A spectral hole is burned at 8 K and its area is measured immediately afterwards. The sample is heated to the cycling temperature T (*e.g.* 40 K), hold there for a few minutes, and finally cooled down back to 8 K; the hole area is then remeasured and compared with the initial value. The whole process is repeated for various cycling temperatures, each time using a new spot on the sample. The solid line corresponds to a fit that is discussed in the text.

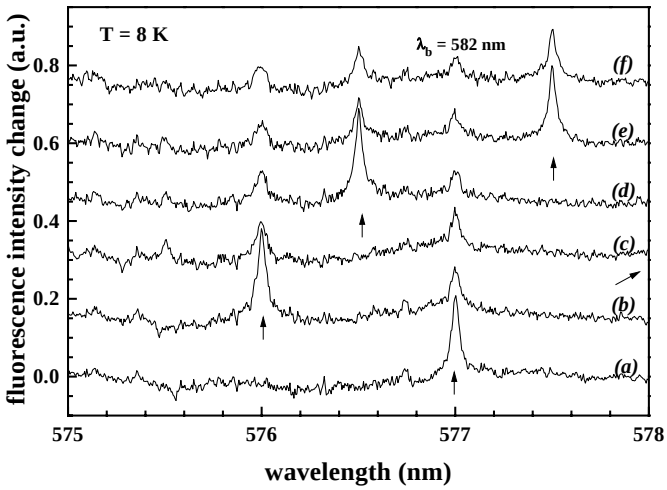

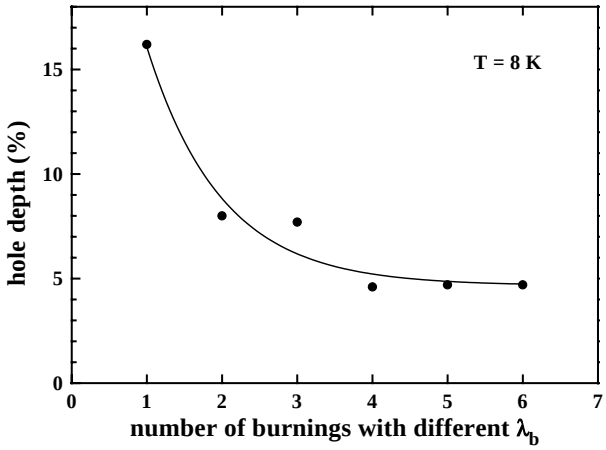

Fig. 7. Light-induced hole refilling studies carried out at 8 K. A spectral hole was burned at 577 nm and the fluorescence excitation spectrum measured afterwards. Without changing the sample position, a second hole was burned at 576 nm and the fluorescence excitation spectrum measured again. The process was repeated, changing the burning wavelength. The upper part shows the successive spectra; for the sake of clarity, they have been vertically translated with respect to one another. The lower part shows the hole depth of the initial 577 nm hole as a function of the number of burnings; the solid line is a guide to the eye.

the spectral position of the new beam with respect to the hole, either blue side or red side, seems to be irrelevant. Even irradiating in the far wings of the band, see curve (f) for example for the effect of 582 nm wavelength irradiation, also leads to refilling. Plotting, as is done in the lower part of Figure 7, the depth of the first hole, at 577 nm, as a function of the number of irradiations leads to a result similar to the one shown in Figure 5.

Using PSHB as a spectroscopic tool, we also studied optical dephasing of the $^7F_0$–$^5D_0$ transition of the Eu^{3+} ion doped in our AlSi glass. A spectral hole was burned, at low irradiation dose in order to decrease the effect of saturation, at 576 nm and 8 K and its width and position were measured as the temperature was increased. As is well-known, the hole width increases with irradiation dose. Ideally, for each temperature, one should measure the hole width for different doses and then extrapolate to zero dose. We chose an irradiation dose such that the corresponding hole width at 8 K did not exceed this extrapolated value by more than 5%; saturation broadening is weaker at higher temperatures. Assuming the laser spectral profile to be Lorentzian, the unsaturated hole width is the sum of the homogeneous linewidth at 8 K plus the homogeneous linewidth at temperature T plus twice the laser spectral width [19]. Figure 8 shows the temperature

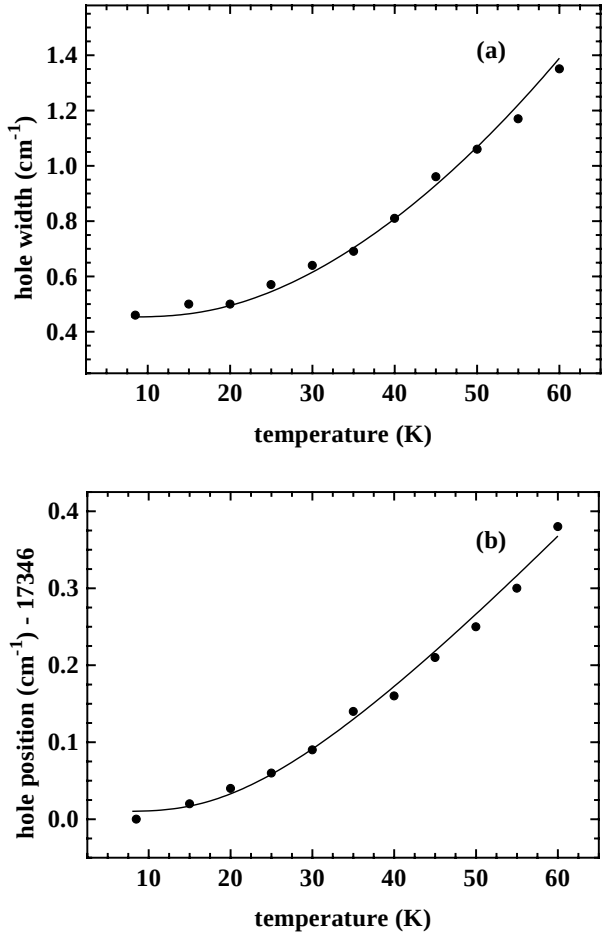

Fig. 8. Temperature dependence of the hole spectral width, part (a), and of the hole central frequency, part (b), in the 8–60 K temperature range. The hole was burned at 8 K and 576 nm. The solid lines correspond to a fit assuming a two-phonon (Raman) process involving pseudo-local phonons of mean frequency ~ 50 cm^{-1}; see text for details.

dependence, in the 8 to 60 K range, of the hole width (Fig. 8a), and of the hole central frequency or, equivalently, of the frequency shift (Fig. 8b).

4 Discussion

Room-temperature PSHB has been observed for the Eu^{3+} ion in a sodium aluminosilicate glass [15] and in a sodium silicate glass [16]. In both cases, holes were burned using a continuous-wave (CW) laser. We observe here room-temperature PSHB for the same ion in a third kind of host, an aluminosilicate glass, using a high peak-power nanosecond laser. Using a CW laser with a 2.5 W/mm^2 intensity, a very similar material had been observed to exhibit PSHB at 77 K, the depth of the hole decreasing to one third of its initial value after storage of the sample at 300 K for 16 hours [14]. One may wonder whether room-temperature PSHB in this AlSi glass host requires a high peak-power laser.

One may think that, if PSHB were a two-photon process, a high peak-power would be more favorable. We first note that it is usually difficult to determine whether PSHB is a single-photon process or a multi-photon one. In the case of photon-gated hole-burning, the situation is clear. In the case of a single laser beam, the burning rate may be determined by a rate-limiting step; if so, the power dependence for a multi-photon process is the same as for a single-photon one. We had in this work indications of a one- (or apparently one-) photon process. We also note that the burning photon energy is 2.15 eV whereas the pseudo-gap of the glass matrix is less than twice this photon energy. Two photons would suffice to ionize our impurities.

We now compare the two situations (pulsed *versus* CW) more quantitatively. Our average intensity, on the order of 2 W/mm^2, is about the same as the one used in reference [14], 2.5 W/mm^2. Assuming a one-photon process, the two situations would be very similar. Assuming a two-photon process and using our pulsed laser with a 2 W/mm^2 average intensity, each laser pulse with a fluence of about 40 mJ/mm^2 would excite part of the Eu^{3+} ions from the ground $^7F_0$ state to the metastable $^5D_0$ level. The same fluence would then drive the photochemical reaction in what would be a self-photon-gated process. Using a CW laser with an intensity of 2.5 W/mm^2 [14], since the lifetime of the $^5D_0$ level is about 1.6 ms, the gating fluence would be 4 mJ/mm^2, only 10 times weaker. Room-temperature PSHB in the AlSi matrix using a CW laser then seems possible. We observe however that, in the measurements performed using a CW laser, the burning intensity was higher in this last host [14] than in sodium aluminosilicate [15] or sodium silicate [16] glass.

4.1 Burning and refilling kinetics, PSHB mechanisms

The mechanisms leading to high-temperature PSHB for the Eu^{3+} ion doped in glasses are still unclear. To date, nobody has been able to observe any absorption feature that could be related to the photoproducts. For Eu^{3+}-doped silicate glass at low temperature, PSHB was shown to be due to optical pumping within the nuclear quadrupole sub-levels of the $^7F_0$ ground state [4]; anti-holes were observed in this case. In higher temperature (110 K) PSHB for Eu^{3+} doped in β''-alumina, it was suggested that the mechanism was a photoinduced rearrangement of the local structure of the host [20]. Such a mechanism had already been suggested in the case of Pr^{3+}-doped silicate glass [4]. For such a non-photochemical mechanism, the total line area is unchanged. As shown in Figure 2, we observe a global decrease for this area, indicating that photoinduced rearrangement of the host local structure is not the unique or dominant mechanism in the case of Eu^{3+}. A similar conclusion was drawn in [16].

The spontaneous refilling kinetics data that are shown in Figure 4 seem to indicate that at least two mechanisms, a slow one and a fast one, are involved in our case,

both at low and room temperature. At low temperature, Figure 4b, a third faster component is observed. The thermal cycling measurements whose results are shown in Figure 6 partly support this conclusion. Thermal cycling results are usually fitted assuming a thermally activated process with a distribution $g(V)$ of barrier heights [20]. This may be readily generalized: the normalized area after cycling at temperature T is then given by:

$$f(T) = 1 - \sum_i \alpha_i \int_0^{k_B T \ln(R_0 t)} g_i(V) \mathrm{d}V \qquad (1)$$

in which R_0 is the attempt frequency, t is the holding time at temperature T, k_B is Boltzmann's constant, α_i is the contribution ($\sum_i \alpha_i = 1$) of the ith mechanism. For a Gaussian distribution:

$$g_i(V) = \left(2\pi\sigma_i^2\right)^{-1/2} \exp\left[-(V - V_i)^2/2\sigma_i^2\right] \qquad (2)$$

V_i being the mean barrier height and σ_i the standard deviation. When the standard deviation is no longer small compared with the mean height, a natural extension of the Gaussian distribution is the log-normal one:

$$g_i(V)\mathrm{d}V = \left[2\pi \left(\sigma_i/V_i\right)^2\right]^{-1/2} \times \exp\left[-\left(\ln(V/V_i)\right)^2/2\left(\sigma_i/V_i\right)^2\right] \mathrm{d}V/V. \qquad (3)$$

The fit in Figure 6 was obtained assuming two distributions. The first one is a log-normal distribution with a mean activation energy $V_1 = 0.12$ eV and a standard deviation $\sigma_1 = 0.07$ eV and could correspond to the fast component(s) in Figure 4. The second one is a Gaussian distribution of mean activation energy V_2 larger than 1.4 eV and would correspond to the slow component. In the fit, we used the value 33 for $\ln(R_0 t)$ for both contributions.

To date, two mechanisms have been suggested to explain PSHB above 4 K in Eu^{3+}-doped glasses: photoinduced rearrangement of the local structure of the host [17,21] as already mentioned and photoinduced reduction of Eu^{3+} to Eu^{2+} [15,16]. Photoinduced reduction of Sm^{3+} to Sm^{2+} has recently been observed in a sodium aluminosilicate glass [22]. In all the reported cases of high temperature PSHB for the Eu^{3+} ion, Eu^{2+} ions were present in a significant amount in the matrix and transfer of an electron from the matrix toward a Eu^{3+} ion or backwards seems to be possible. In the present work in which we observe a fast or "easy" and a slow component, we may imagine that the low-barrier one is either a local rearrangement of the host or a photoreduction process. We may wonder how photoreduction is possible since the excited electron belongs to the $4f$ sub-shell of the Eu^{3+} ion whereas the chemical process is the transfer of an electron from the glass matrix to the same ion. One possibility is that the ground $^7F_0$ state of the Eu^{3+} ion be located beneath the top of the pseudo-valence band of the matrix, the excited $^5D_0$ state being located in the gap. Absorption of a photon would then create an acceptor site that would capture an electron from the pseudo-valence band. Europium would then be present as an excited Eu^{2+} ion eventually relaxing to its ground state.

We suggest that the slow PSHB mechanism, that corresponds to a much higher activation energy, involves several steps. First, a two-photon process would lead to ionization of Eu^{3+} to Eu^{4+}. Second, the ejected electron would be trapped, possibly on a Eu^{3+} site: this would explain the overall decrease of the line shown in Figure 2. Third, its local environment would reduce the Eu^{4+} ion created in the first step; the Eu^{3+} site thus created would possess a very different environment and its absorption line would be strongly shifted. In the case of Pr^{3+}:YAG, the PSHB mechanism was suggested to be two-photon ionization of Pr^{3+} to Pr^{4+} [23]. Praseodymium is known to exist with either of these valences. Eu^{4+} on the other hand does not seem to be stable. The mechanism we suggest here then amounts to an electron transfer from a Eu^{3+} site to another (distant) one. In this target site, the extra electron would rather be located around the Eu nucleus. In the original site, the hole (missing electron) would rather be located in the local glass environment.

Within this frame, the first two mechanisms, either local rearrangement of the host or photoreduction, would explain the relatively easy and fast spontaneous refilling of part of the hole. Since the thermal properties of glasses are almost normal above a few kelvins (regarding the thermal properties of glasses or those of mixed crystals, we refer the reader to [24]), this means that the potential barriers hindering structural rearrangement often have a moderate height. In the same way, the presence of a significant number of Eu^{2+} ions indicates that a small amount of energy is needed to transfer an electron from the host to Eu^{3+} or *vice versa*. Assuming a broad distribution for the height of potential barriers, this would explain why such "easy" processes may be involved in such a broad temperature range, although less so at room temperature (the maximum hole depth decreases from 20% at 8 K to 5% at 295 K). At low temperature, as shown in Figure 4b, both a fast and a faster components can be seen. They may correspond to the two "easy" mechanisms discussed above. It is presently unclear which one would lead to the most stable products. Regarding Figure 6, the broad barrier height distribution may describe both "easy" processes.

The process we suggest for the slow mechanism would be much less reversible. It requires a highly improbable electron transfer over a sizable distance. The activation energy for the backward as well as for the forward reaction is certainly higher than the ionization energy. This would explain the slow component in the refilling kinetics.

Regarding Figure 3, the constant term in the fit corresponds to the maximum hole depth one can burn. The burning kinetics data then apparently show only one component. This may be understood in the following way. We start with N_0 ions in the ground state. The burning laser takes part of them to an excited level from which a fraction η_1 decays to the "trap" level 1 and a fraction η_2 to another "trap" level 2 (for simplicity, we assume two processes). The numbers N_1 and N_2 of ions occupying

levels 1 and 2 obey the rate equations:

$$\frac{\mathrm{d}N_1}{\mathrm{d}t} = W_1(N_0 - N_1 - N_2) - \frac{N_1}{\tau_1} \quad (4)$$

$$\frac{\mathrm{d}N_2}{\mathrm{d}t} = W_2(N_0 - N_1 - N_2) - \frac{N_2}{\tau_2} \quad (5)$$

where W_1 and W_2 are the excite-and-trap rates and τ_1 and τ_2 the lifetimes for the two trap levels respectively. W_1 and W_2 are respectively proportional to η_1 and η_2 and depend on the burning laser intensity in the same way (for example linearly for a one-photon process). The factor $(N_0 - N_1 - N_2)$ is the number of ions that are still present in the ground state at time t. Now, for the fast component, τ_1 is $\sim$ 2 hours and, for the slow one, τ_2 is much longer. On the time-scale of the burning kinetics measurements, Figure 3, the last terms in equations (4, 5) may be neglected. Adding the two equations, we get for the total number of ions missing in the ground state the simple rate equation:

$$\frac{\mathrm{d}(N_1 + N_2)}{\mathrm{d}t} = (W_1 + W_2)(N_0 - N_1 - N_2) \quad (6)$$

leading to a single exponential component for the time dependence of the hole depth. In fact only a certain fraction (N_0) of the ions take part in the process.

Regarding light-induced hole refilling, the "easy" mechanisms only require a weak photoexcitation in order to move backwards. This would explain why the spectral position of the "erasing" beam with respect to the hole, either blue side or red side, either central or in the wings is of little relevance. We also observe that this fact indicates that non-radiative energy transfer between optical centers is not responsible for hole refilling. The slow mechanism, with a higher activation energy, should require excitation of Eu^{2+} ions. But these ions have a very broad absorption spectrum. This too would be consistent with the large insensitivity of light-induced hole refilling to the frequency of the "erasing" beam.

4.2 Optical dephasing

Before discussing the results shown in Figure 8 regarding the line broadening mechanisms, we first consider a point raised by another (extreme) site-selective technique, single molecule spectroscopy (SMS). Is "homogeneous width" a meaningful concept in a glass matrix, especially at low temperature? SMS [25] has shown that the position and width of the fluorescence spectrum of a single molecule change with time. The (time average) linewidth is usually obtained from a Lorentzian fit to the experimental data but, assuming a TLS mechanism, it has recently [26] been shown theoretically that the SMS spectrum is usually not Lorentzian. And the distribution of widths obtained using SMS does not necessarily coincide with the width measured using more conventional techniques such as photon echo. This is related to the basic ergodicity problem in statistical physics. It has been argued that, at low temperature, glasses are non-ergodic systems [27]. The ion-environment interaction changes from site to site in its static or time-average part: this causes inhomogeneous broadening. But it is also expected to change in its dynamic part, the one causing dephasing. At low temperature, broadening is not the same everywhere in the sample, it is not *homogeneous*.

The above considerations pertain to the low temperature case. As already pointed out above, the thermal properties of glasses are back to normal above a few kelvins [24] and such non-ergodicity problems should have disappeared. When discussing the results shown in Figure 8, that were obtained in the 8 to 60 K temperature range, we will deliberately assume that such is this case. In this high temperature range, experimental results for the homogeneous linewidth in glassy hosts show a quasi-universal quadratic temperature dependence [28] although an Arrhenius-type dependence has also been reported [18]. In order to interpret these results, several processes or models have been discussed: TLS [1], the exchange model [18], acoustic phonons [29], non-Debye phonons [29–34] and fractons [35]. The role of TLS in line broadening has been extensively considered (see for example Ref. [2]) and seems to be important only below a few kelvins. We then expect that, in our case, TLS play a minor role. As will become clear below, in our case, the main line broadening contribution is indeed observed to originate in non-Debye phonons.

The role of phonons in line broadening of electronic transitions of impurities doped in a crystalline matrix is a well-documented subject [36]. It has recently been reconsidered within the general framework of relaxation theory with particular emphasis on the connection that sometimes exists between the linewidth and the frequency shift [37]. In the present work, due to the long lifetime of the $^5D_0$ and $^7F_0$ levels, lifetime broadening is negligible and line broadening is due to pure dephasing processes. In the case of phonon broadening, pure dephasing is due to two-phonon (Raman) processes. The corresponding contributions to the temperature-dependent part of the homogeneous linewidth Γ and of the frequency shift $\Delta\nu$ are given by:

$$\Gamma = \beta \int [\rho(\omega)\omega]^2 p_0(\omega)[p_0(\omega) + 1]\mathrm{d}\omega \quad (7)$$

$$\Delta\nu = \beta' \int \rho(\omega)\omega p_0(\omega)\mathrm{d}\omega \quad (8)$$

where $\rho(\omega)$ is the phonon density of modes and $p_0(\omega) = 1/[\exp(\hbar\omega/k_\mathrm{B}T) - 1]$ is the mean phonon number for a mode of angular frequency ω at temperature T. The expressions for the β and β' coefficients may be found in [37]. The nature of the phonons involved may change from one case to the other. In glassy matrices, it has been argued [38] that low-frequency long-wavelength acoustic phonons still exist but that, due to the lack of translational invariance, higher frequency modes are localized modes. It is still unclear however whether the boson peak corresponds to localized vibrational modes or not [3]. Independent evidence for the role of low-frequency, non-Debye,

vibrational modes of the glass matrix in the electron-phonon coupling Hamiltonian has also been reported [39,40]. In this paper, we will term these non-Debye modes pseudo-local phonons. In the case of vitreous silica, they have been assigned to rotations of SiO_4 tetrahedra [41]. As can be seen in Figure 8, our experimental data for the temperature dependence of both the homogeneous linewidth and frequency shift can be fitted according to equations (7, 8) assuming a narrow pseudo-local phonon distribution centered around $\sim$ 50 cm^{-1} for the spectral density of modes. These phonon frequencies are close to frequencies of vibrations obtained experimentally in [41]. The fit in Figure 8 was obtained assuming a Gaussian density of modes with a mean frequency of 50 cm^{-1} and a 7 cm^{-1} standard deviation.

In the case of such a narrow peak, the temperature dependencies of the linewidth and of the frequency shift are dominated by the factors $p_0(\omega_0)[p_0(\omega_0)+1]$ and $p_0(\omega_0)$ respectively, where ω_0 is the mean angular frequency. We observe that, in the low temperature case, they both vary as $\exp(-\hbar\omega_0/k_BT)$, the Arrhenius-type behavior reported in [18]. We may wonder why pseudo-local phonons would be more efficient than acoustic phonons in the optical dephasing process. They may differ in the density ρ, but also in the β and β' coefficients that appear in equations (7, 8). Assuming pseudo-local phonons to correspond to localized modes, one would expect them to lead to strains having larger spatial frequency components and thus a more efficient change in the crystal field (at the location of the Eu^{3+} ion) than long wavelength acoustic phonons. This was already discussed in [38] and may of course depend on the material under study.

The contribution of Raman processes vanishes at low temperature. The origin of the low temperature homogeneous width is presently unknown. It could be due to TLS. We observed that this low-temperature homogeneous linewidth increases roughly linearly when the transition frequency increases across the inhomogeneous profile. Fluorescence line narrowing measurements have shown that the magnitude of the static part of the crystal field also increases linearly [42]. We may expect the dynamic part of the crystal field to behave in the same way. Such a similarity has been observed in a silicate glass matrix [43].

5 Conclusion

To summarize, we have observed room-temperature persistent spectral hole-burning for the Eu^{3+} ion doped in an aluminosilicate glass matrix. Long-lived, 5% deep, persistent holes could be burned in the $^7F_0$–$^5D_0$ line using a nanosecond high peak-power dye laser. High-temperature PSHB cannot be observed in a pure silicate matrix [21,43]. It has already been pointed out that introduction of Al^{3+} ions in silicate glass promotes the formation of stable spectral holes [21]. Our observations tend to support such a statement but we note that, according to recent work [15,16], other network modifier cations may also prove promising. In all cases of high-temperature PSHB for the Eu^{3+} ion, a significant amount of Eu^{2+} ions are present in the matrix indicating that the glass host is electron donating.

Comparing our results with previous work, we have discussed the possibility of using a continuous-wave laser. Studies of spontaneous refilling kinetics performed at room and at low temperature as well as thermal cycling measurements show that two mechanisms at least are at play: a fast or "easy" one may involve non-photochemical local rearrangement of the host or a photoinduced reduction process. In order to explain the second (slower and much less reversible) component, we suggest a three-step process amounting to electron transfer over a sizable distance, the electron in the target site being located near a Eu nucleus and the subsequent hole created in the original site being more probably located in the glass host. These findings and suggestions agree with light induced hole refilling measurements. They also allow us to understand the exponential growth of the hole depth in the burning kinetics study.

Assuming "homogeneous broadening" to be a meaningful concept, the temperature dependence of the homogeneous width as well as that of the corresponding frequency shift could be interpreted in terms of a two-phonon (Raman) process involving pseudo-local phonons of mean frequency 50 cm^{-1}. At room temperature and because of saturation effects, the observed hole width of 3.2 cm^{-1} is only an upper limit implying a lower limit of 50 for the enhancement factor related to frequency selective optical data storage.

References

1. P.M. Selzer, D.L. Huber, D.S. Hamilton, W.M. Yen, M.J. Weber, Phys. Rev. Lett. **36**, 813 (1976).
2. E. Geva, J.L. Skinner, J. Chem. Phys. **107**, 7630 (1997) and references therein.
3. T. Uchino, T. Yoko, J. Chem. Phys. **108**, 8130 (1998); D. Engberg, A. Wischnewski, U. Buchenau, L. Börjesson, A.J. Dianoux, A.P. Sokolov, L.M. Torell, Phys. Rev. B **59**, 4053 (1999).
4. R.M. Macfarlane, R.M. Shelby, Opt. Commun. **45**, 46 (1983).
5. R.M. Macfarlane, R.M. Shelby, Opt. Lett. **9**, 533 (1984).
6. W.S. Brocklesby, B. Golding, J.R. Simpson, Phys. Rev. Lett. **63**, 1833 (1989).
7. See for example W.E. Moerner, *Persistent Spectral Hole-Burning: Science and Applications* (Springer-Verlag, Berlin, 1988).
8. B. Plagemann, F.R. Graf, S.B. Altner, A. Renn, U.P. Wild, Appl. Phys. B **66**, 67 (1998).
9. R. Jaaniso, H. Bill, Europhys. Lett. **16**, 569 (1991).
10. J. Zhang, S. Huang, J. Yu, Opt. Lett. **17**, 1146 (1992).
11. K. Holliday, C. Wei, M. Croci, U.P. Wild, J. Lumin. **53**, 227 (1992).
12. K. Hirao, S. Todoroki, D.H. Cho, N. Soga, Opt. Lett. **18**, 1586 (1993).
13. K. Hirao, S. Todoroki, K. Tanaka, N. Soga, T. Izumitani, A. Kurita, T. Kushida, J. Non-Cryst. Solids **152**, 267 (1993).
14. Y. Mao, P. Gavrilovic, S. Singh, A. Bruce, W.H. Grodkiewicz, Appl. Phys. Lett. **68**, 3677 (1996).

15. K. Fujita, K. Tanaka, K. Hirao, N. Soga, Opt. Lett. **23**, 543 (1998).
16. K. Fujita, K. Tanaka, K. Hirao, N. Soga, J. Opt. Soc. Am. B **15**, 2700 (1998).
17. M. Nogami, Y. Abe, J. Opt. Soc. Am. B **15**, 680 (1998).
18. S. Voelker, R.M. Macfarlane, J.H. van der Waals, Chem. Phys. Lett. **53**, 8 (1978).
19. W. Beck, D. Ricard, C. Flytzanis, Phys. Rev. B **58**, 11996 (1998).
20. H. Yugami, R. Yagi, S. Matsuo, M. Ishigame, Phys. Rev. B **53**, 8283 (1996).
21. K. Fujita, K. Hirao, K. Tanaka, N. Soga, H. Sasaki, J. Appl. Phys. **82**, 5114 (1997).
22. J. Qiu, K. Miura, T. Suzuki, T. Mitsuyu, K. Hirao, Appl. Phys. Lett. **74**, 10 (1999).
23. R.M. Macfarlane, G. Wittmann, Opt. Lett. **21**, 1289 (1996).
24. D.G. Cahill, R.O. Pohl, Phys. Rev. B **39**, 10477 (1989) and references therein.
25. J.L. Skinner, W.E. Moerner, J. Phys. Chem. **100**, 13251 (1996).
26. E. Geva, J.L. Skinner, J. Phys. Chem. **101**, 8920 (1997).
27. F.H. Stillinger, Science **225**, 983 (1984).
28. See for example W.M. Yen, in *Laser Spectroscopy of Solids II*, edited by W.M. Yen (Springer-Verlag, Berlin, 1989), p. 10.
29. S.N. Gladenkova, I.S. Osad'ko, Chem. Phys. Lett. **187**, 628 (1991).
30. J. Hegarty, W.M. Yen, Phys. Rev. Lett. **43**, 1126 (1979).
31. I.S. Osad'ko, JETP Lett. **33**, 626 (1981) [Pis'ma Zh. Eksp. Teor. Fiz. **33**, 640 (1981)]; I.S. Osad'ko, S.A. Zhdanov, Opt. Commun. **42**, 185 (1982).
32. D.L. Huber, J. Non-Cryst. Solids **51**, 241 (1982).
33. D.L. Huber, J. Lumin. **36**, 327 (1987).
34. R. Yano, M. Mitsunaga, N. Uesugi, M. Shimizu, Phys. Rev. B **50**, 9031 (1994).
35. F. Durville, G.S. Dixon, R.C. Powell, J. Lumin. **36**, 221 (1987).
36. W.M. Yen, W.C. Scott, A.L. Schawlow, Phys. Rev. **136**, A271 (1964).
37. W. Beck, D. Ricard, C. Flytzanis, Phys. Rev. B **57**, 7694 (1998).
38. G. Dixon, P.A. Watson, J.P. Wicksted, D. Bromwell, J. Lumin. **60/61**, 430 (1994).
39. D.W. Hall, S.A. Brawer, M.J. Weber, Phys. Rev. B **25**, 2828 (1982).
40. F.J. Bergin, J.F. Donegan, T.J. Glynn, G.F. Imbush, J. Lumin. **34**, 307 (1986).
41. U. Buchenau, N. Nuecker, A.J. Dianoux, Phys. Rev. Lett. **53**, 2316 (1984) and erratum, *ibid.* **56**, 539 (1986); U. Buchenau, M. Prager, N. Nuecker, A.J. Dianoux, N. Ahmad, W.A. Phillips, Phys. Rev. B **34**, 5665 (1986).
42. G. Nishimura, T. Kushida, J. Phys. Soc. Jpn **60**, 695 (1991).
43. T. Schmidt, R.M. Macfarlane, S. Voelker, Phys. Rev. B **50**, 15707 (1994).